Pore-scale Simulations On The Impacts Of Hydrate Production Approaches On Gas And Water Transport In Hydrate-bearing Sediments

Zhuoran Li, Guan Qin

University of Houston

Outline

- Background and motivation
- Lattice Boltzmann(LB) method
- LB model for multiphase reactive transport processes
  - Model verification
  - Simulation study on relative permeability estimation during hydrate dissociation
- Conclusion

Background and motivation

- Gas hydrates resource
  - Hydrates are crystalline compounds composed of gas molecules trapped in a lattice of water molecules
  - Stable under low temperature and high pressure
  - Over 3000 trillion cubic meters
- Production challenges associated with permeability changes
  - Gas surge in production
  - Excessive water production
  - Economic feasibility

(Wikipedia: Methane hydrate)

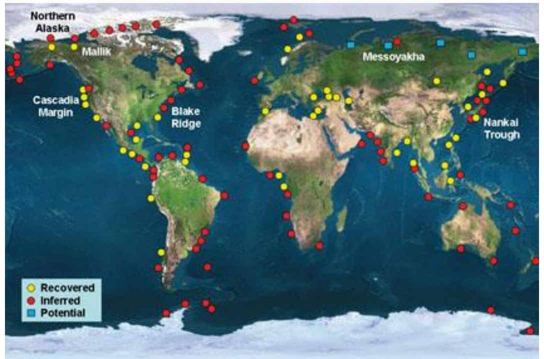

(Boswell et al. , 2009)

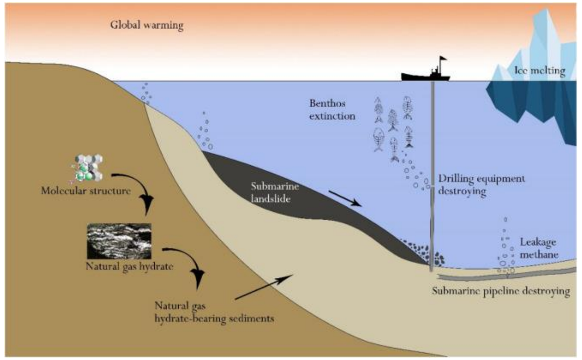

(Ren, X. et al., 2020)

Hydrate dissociation processes

- Essential physicochemical processes during hydrate dissociation
  - Dissociation reaction of methane hydrate: $\mathrm{CH_4 \cdot 5.75H_2O \rightarrow CH_4 \uparrow + 5.75H_2O}$
    - Triggered by changes in temperature/pressure conditions
    - Endothermic, self-inhibition reaction
  - Evolution of pore structure during dissociation
  - Fluids transport through the interconnected network of pores
  - Heat transfer from artificial heat source/ sensible heat in adjacent layers

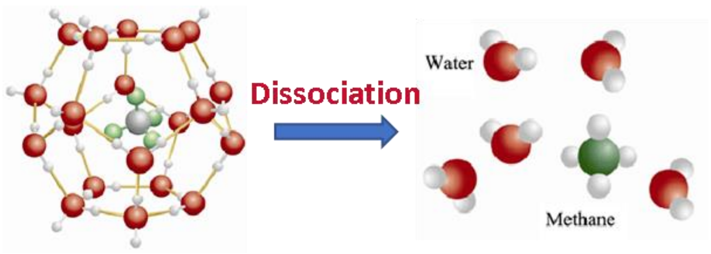

(Lee, J. Y. et al.,2011)

Dissociation

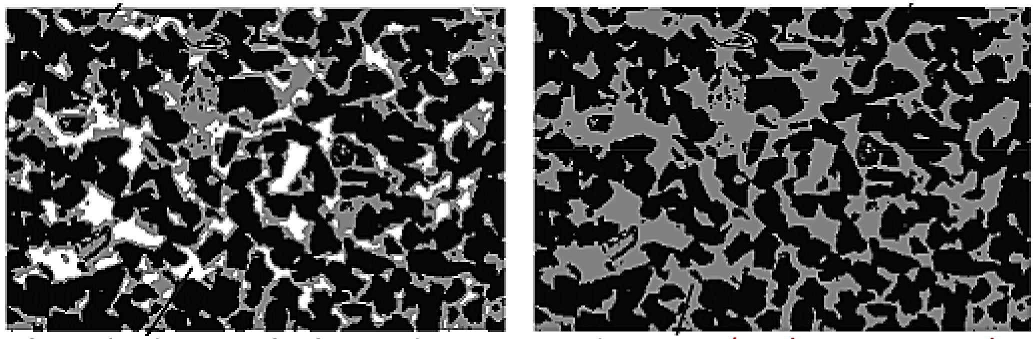

White: hydrate; **Black**: sand; **Grey**: void space (Malinverno et al.,2008)

Evolution of pore structure

(MH21-S R&D consortium)

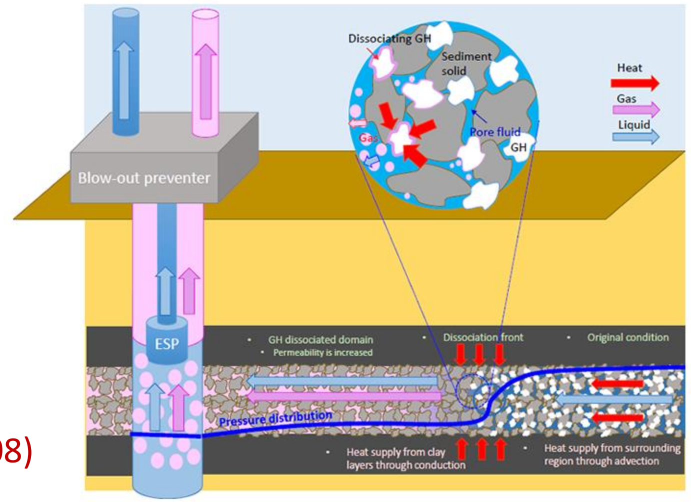

Hydrate production

Methodology selection

- Lattice Boltzmann simulation for reactive transport and permeability estimation
  - Flexibility in boundary conditions treatment
    - Handle complex pore geometries
    - Capture pore scale interactions between fluids and solids
  - Reliable numerical stability
  - Ease of implementation and efficient parallelization

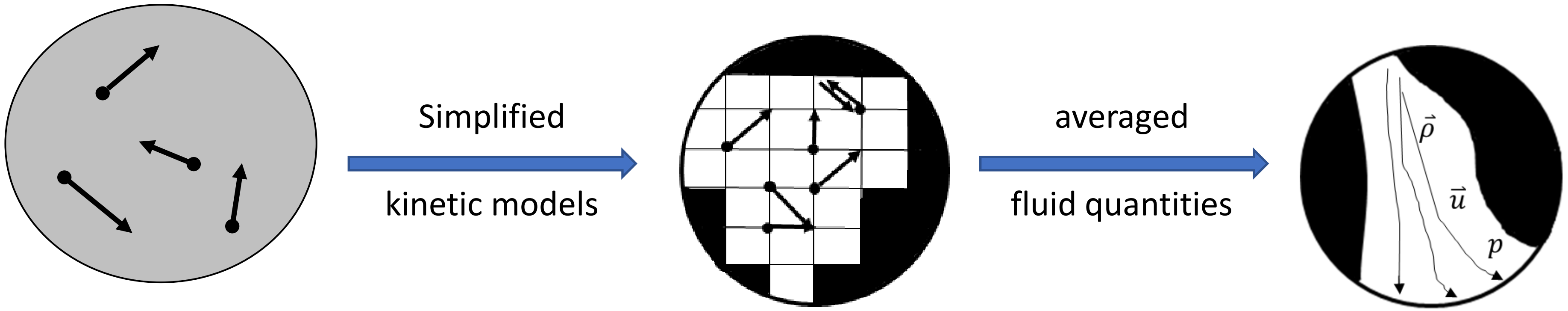

Molecular Dynamics
molecule movement

LB method
particle distributions

N-S equation
macroscopic quantities

InterPore

Lattice Boltzmann model

- Multiphase hydrodynamic LB model
  - Phase field multiphase model (Jacqmin, D, et al., 1999)
    - ➢ Derived by minimizing the Gibbs free energy of the multiphase system to predict phase interface evolutions
    - ➢ Applies the advection-diffusion form of equation to describe the evolution of phase index
    - ➢ Introduces diffuse interfaces between different phases to achieve a smooth transition of physical properties
  - Phase field LB model (Geier, M., et al. 2015)

Phase index distribution

$$h_i(\mathbf{x}+\mathbf{e}_i\Delta t, t+\Delta t) = h_i(\mathbf{x},t) - \frac{h_i(\mathbf{x},t) - \overline{h_i^{eq}}(\mathbf{x},t)}{\tau_\varphi} + S_i^\varphi(\mathbf{x},t)\Delta t$$

$\mathbf{u}$

Pressure distribution

$$f_i(\mathbf{x}+\mathbf{e}_i\Delta t, t+\Delta t) = f_i(\mathbf{x},t) - \frac{f_i(\mathbf{x},t) - \overline{f_i^{eq}}(\mathbf{x},t)}{\tau_f} + S_i(\mathbf{x},t)\Delta t$$

$\rho(\varphi)$

$F_{\text{tot},i}\ (\varphi)$

  - Source term due to dissociation and forces (Verdier, W., et al., 2020)

$$S_i^\varphi(\mathbf{x},t) = F^\varphi{}_{\text{tot},i} + \dot{m}_i{}^\varphi$$

Ensure the surface tension is correctly accounted at interfaces (first term); **Mass source contribution to phase index** (second term)

$$S_i(\mathbf{x},t) = F_{\text{tot},i} + \dot{m}_i$$

Body force, viscous force, surface tension (first term); **Mass source contribution to pressure** (second term)

Lattice Boltzmann model

- Multiphase hydrodynamic LB model
  - Equivalent macroscopic multiphase model (Geier, M., et al. 2015)

$$\frac{\partial \rho}{\partial t} + \nabla \cdot (\rho \mathbf{u}) = \dot{m}$$

$$\frac{\partial \rho \mathbf{u}}{\partial t} + \nabla \cdot (\rho \mathbf{u}\mathbf{u}) = -\nabla p + \nabla \cdot \left(\rho \vartheta (\nabla u + (\nabla u)^T)\right) + F_{\text{tot}} + \dot{m}\mathbf{u}$$

Hydrodynamic equations

$$\frac{\partial \varphi}{\partial t} + \nabla \cdot (\varphi \mathbf{u}) = \nabla \cdot \left(M_\varphi \left(\nabla \varphi - \frac{4}{W} \varphi (1 - \varphi) \mathbf{n} \right) \right) + \frac{\dot{m}^\varphi}{\rho}$$

Volume diffusive term

Phase index equation (Allen-Cahn equation) (Allen, S. M., et al., 1979)

Lattice Boltzmann model

- Heat transfer LB model
  - Heat transfer equation

Temperature distribution

$$g_i(\mathbf{x} + c\mathbf{e}_i\Delta t, t + \Delta t) = g_i(\mathbf{x}, t) - \frac{1}{\tau_{g,k}}[g_i(\mathbf{x}, t) - g_i^{eq}(\mathbf{x}, t)] + \Delta t \mathrm{F}_i$$

  - Heat source due to latent heat of dissociation and conjugate condition treatment (Karani et al., 2015) (Moridis, 2012)

$$\mathrm{F}_i = \omega_i\left(S_{\mathrm{conj}} + S_{\mathrm{latent}}\right)$$

  - Equivalent macroscopic heat transfer equation (Karani et al., 2015)

$$\rho h \frac{\partial T}{\partial t} + \nabla \cdot (\rho h \mathbf{u} T) = \nabla \cdot (k \nabla T) + S_{\mathrm{latent}}$$

- Geometry alteration model (volume of pixel) (Kang et al., 2006)

VOP

$$V_s(t + \Delta t) = V_s(t) - A V_m S_{\mathrm{reaction}}$$

Multiphase transport model verification

- Verification on hydrodynamic processes
  - Multiphase flow in porous medium (Aursjø et al., 2011)

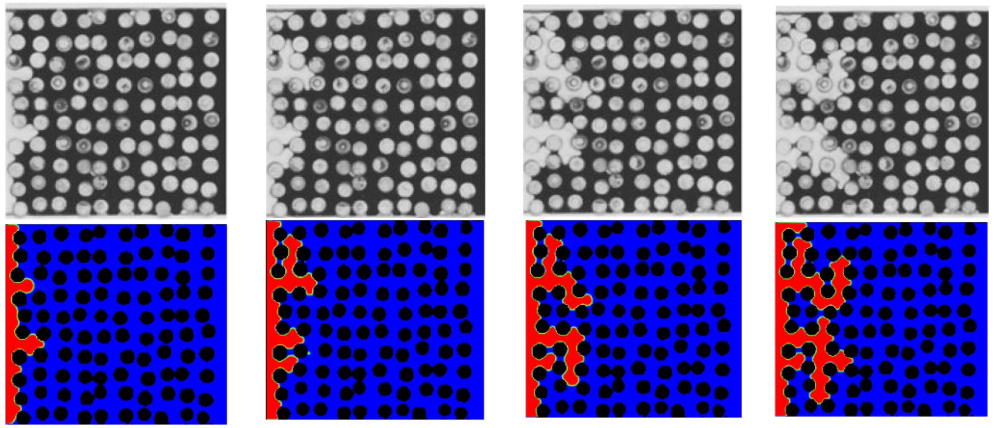

$\frac{t}{t_{bt}} = 0.088$ $\frac{t}{t_{bt}} = 0.224$ $\frac{t}{t_{bt}} = 0.349$ $\frac{t}{t_{bt}} = 0.478$

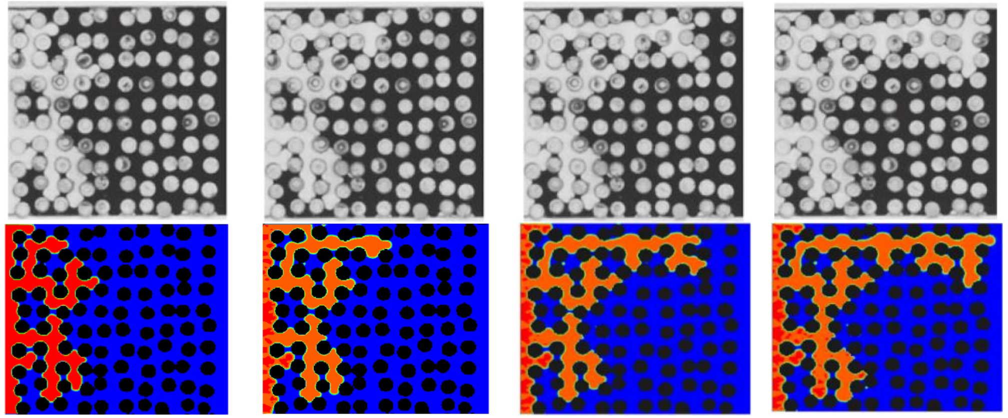

$\frac{t}{t_{bt}} = 0.612$ $\frac{t}{t_{bt}} = 0.740$ $\frac{t}{t_{bt}} = 0.869$ $\frac{t}{t_{bt}} = 1.01$

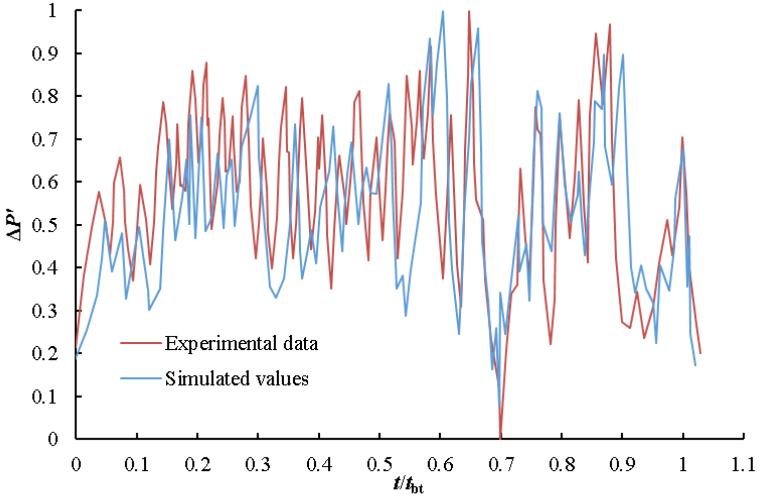

Pressure comparisons

Heat transfer model verification

- Verification on heat transfer processes

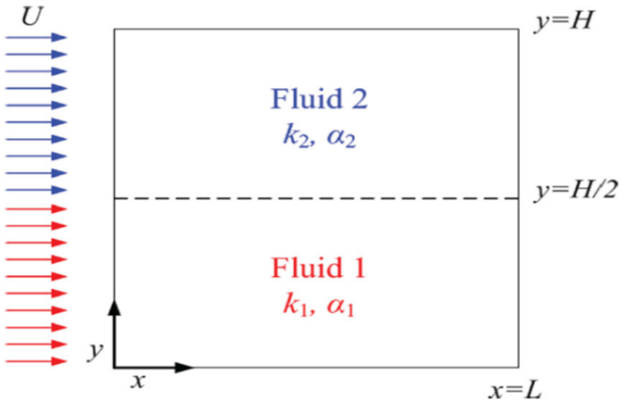

Horizontal walls have fixed sinusoidal temperatures:

$$T(x, y = 0) = T(x, y = H) = \cos(\omega x)\,, \omega = 2\pi/L$$

(Karani et al., 2015)

Steady-state convection-diffusion heat transfer

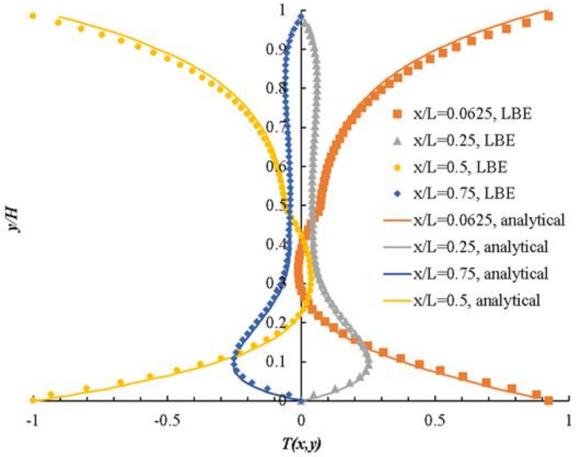

y/H (vs) T

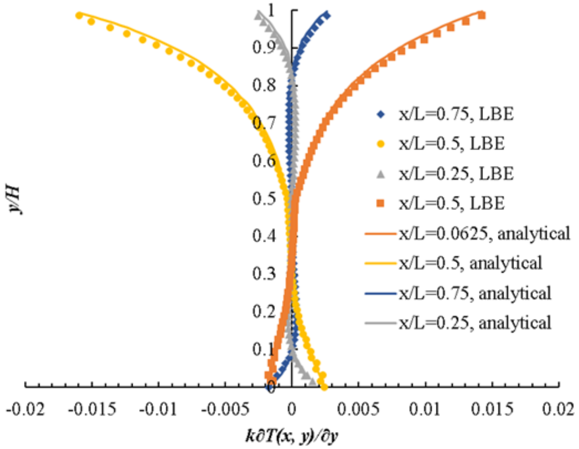

y/H (vs) $k\partial T(x, y)/\partial y$

Simulation for gas and water transport processes

- Simulation setup
  - Evolution of pore structure defines the relative permeability(K_{r}) vs wetting-phase (water) saturation (S_{w}) relation
  - Coupling between fluid transport and heat transfer plays a dominant role in pore structure evolution
  - Study the coupling effects on the $K_{\mathrm{r}} - S_{\mathrm{w}}$ relations on homogeneous hydrate-bearing sediment with two common distribution morphologies under different dissociation conditions

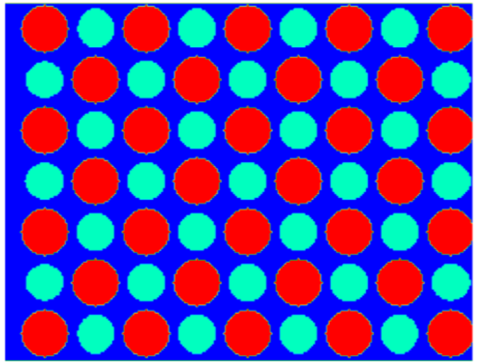

Pore-filling

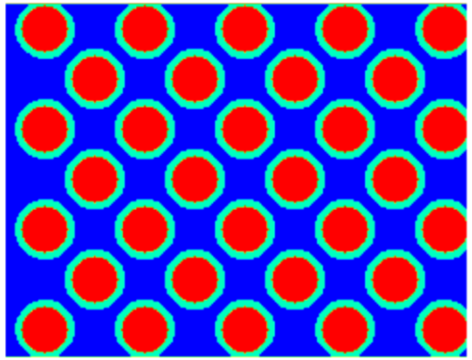

Grain-coating

S_{hyd}=35%
2.42 mm ×1.84 mm
484 × 368
P=12MPa
T=287.75 K

InterPore

Simulation for gas and water transport processes

- Relative permeability estimation during hydrate dissociation
  - Baseline case: isothermal LB simulation on fluid transport
  - Pore structure evolution during dissociation is modeled by assumed evolution patterns
  - Boundary conditions
    - ➢ Periodic boundary condition on outer boundaries
    - ➢ Bounce-back boundary condition on fluid-solid interfaces
    - ➢ Wettability boundary condition on solid boundaries (water contact angle on solid interface: 0°) (Dai, S., et al., 2019)

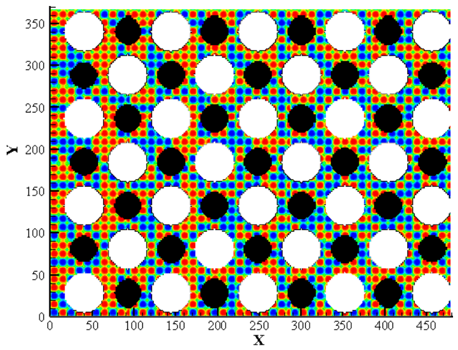

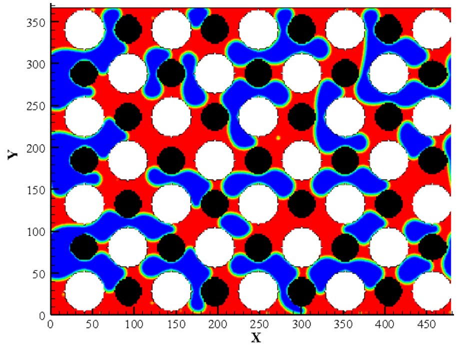

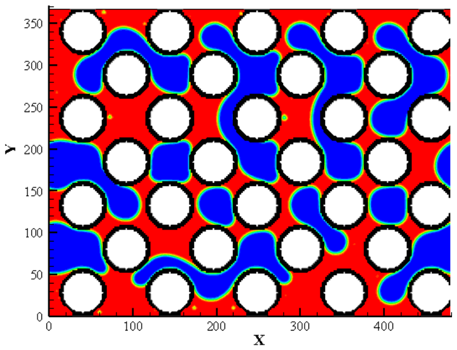

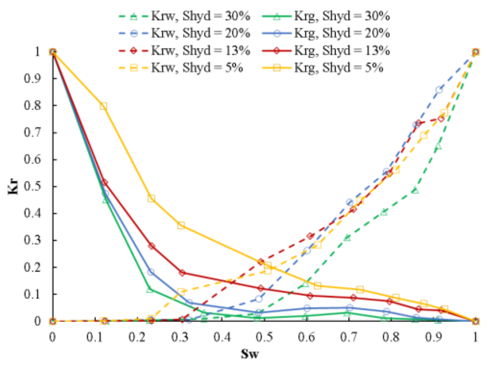

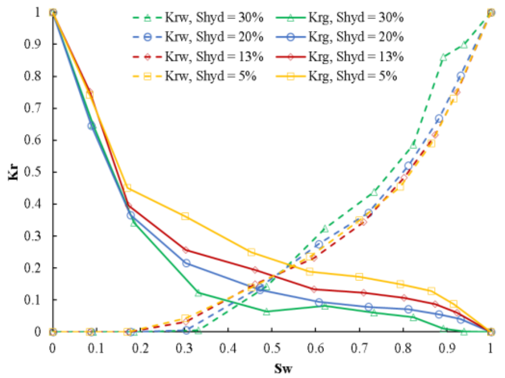

S_{hyd}=20%

Pore filling | Grain-coating

Initialization | Pore filling | Grain-coating | K_{r} vs S_{w}

Simulation for gas and water transport processes

- Relative permeability estimation during hydrate dissociation
  - Thermal stimulation case: both considering latent heat and heat source
  - Top/bottom thermal intervention from hydrate-free layer was considered
  - Boundary conditions
    - Periodic boundary condition on outer boundaries
    - Bounce-back boundary condition on fluid-solid interfaces
    - Constant temperature boundary condition on top/bottom boundaries
    - Fully developed temperature boundary condition on inlet/outlet boundaries
    - Wettability boundary condition on solid boundaries

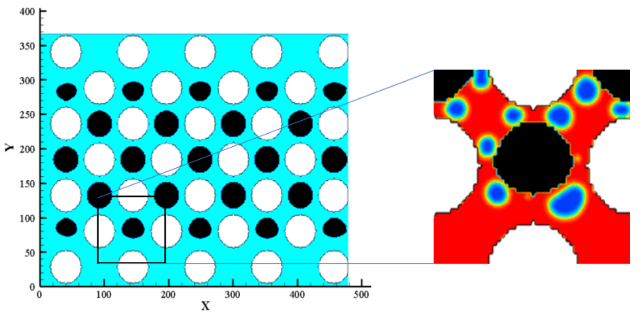

Gas generation during dissociation

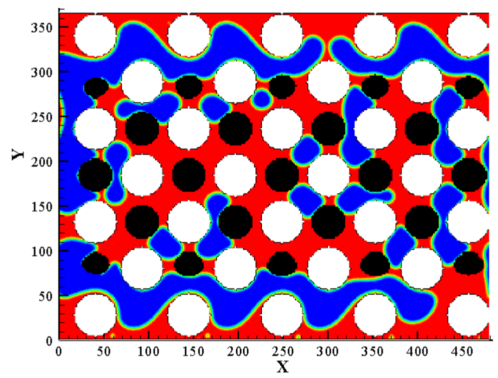

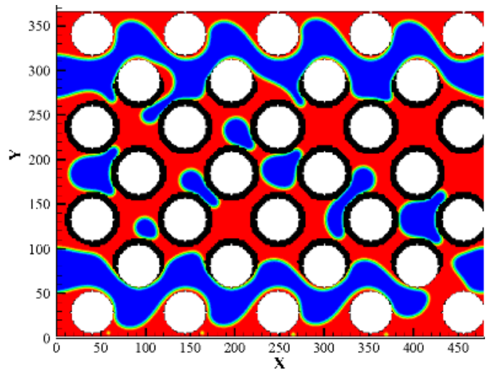

S_{hyd}=20%

Pore filling

Grain-coating

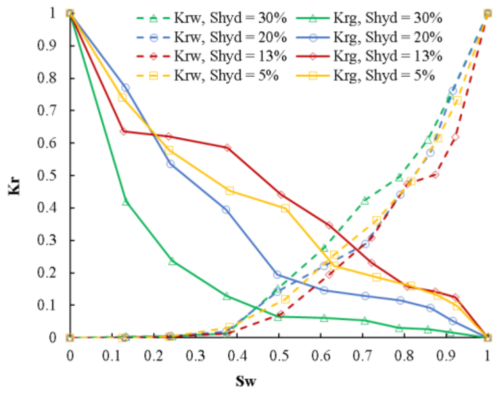

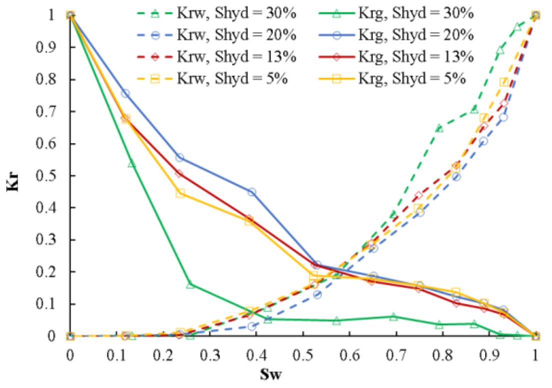

K_{r} vs S_{w}

Simulation for gas and water transport processes

- P_c vs S_w relation comparisons for homogeneous cases
  - P_c vs S_w relations under different hydrate saturation
  - Boundary conditions
    - Constant pressure boundary condition on inlet boundary
    - Convective outflow boundary condition on outlet boundary

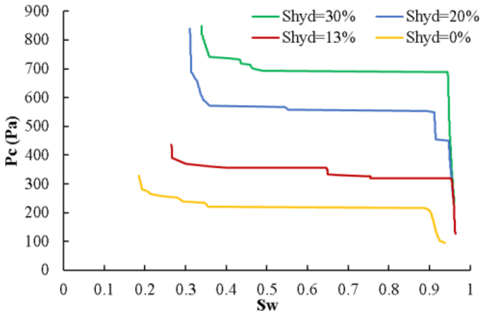

Pore-filling

P_c vs S_w

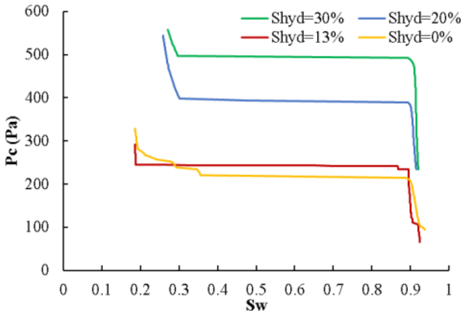

Grain-coating

  - Jamin effect
    - resistance to fluid flow through capillaries which is due to the presence of bubbles/droplets

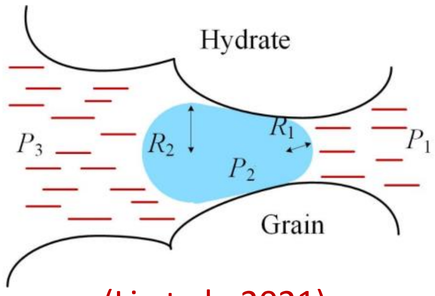

(Li et al., 2021)

$$P_2 - P_1 = \frac{2\sigma_{wg}}{R_1}$$

$$P_2 - P_3 = \frac{2\sigma_{wg}}{R_2}$$

$$P_3 - P_1 = 2\sigma_{wg}\left(\frac{1}{R_1} - \frac{1}{R_2}\right)$$

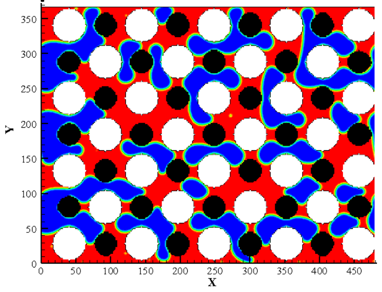

Baseline

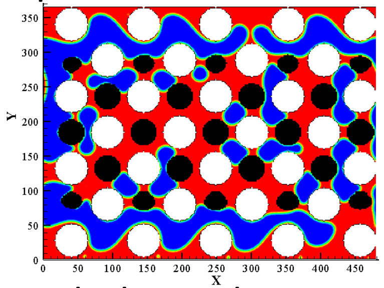

With thermal intervention

Simulation for gas and water transport processes

- K_{r} vs S_w relation comparisons for homogeneous cases
  - Gas gathers in areas without hydrates, while water remains in areas with hydrates due to capillarity
    - The non-wetting phase tends to occupy larger pores, whereas the wetting phase is more likely to occupy smaller pores
    - Gas exhibits lower dynamic viscosity than water, resulting in higher mobility
    - Capillary pressure and Jamin effect are significantly decreased
  - Thermal stimulation cases show considerable improvements in K_{rg} values but little decrease in K_{rw}

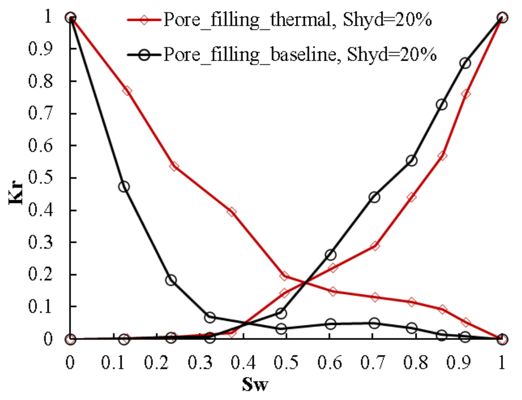

S_{hyd}=20%

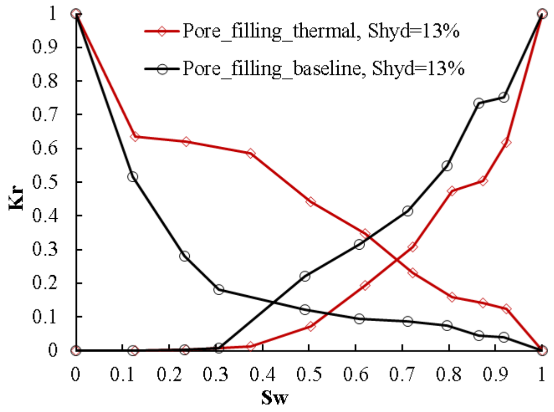

S_{hyd}=13%

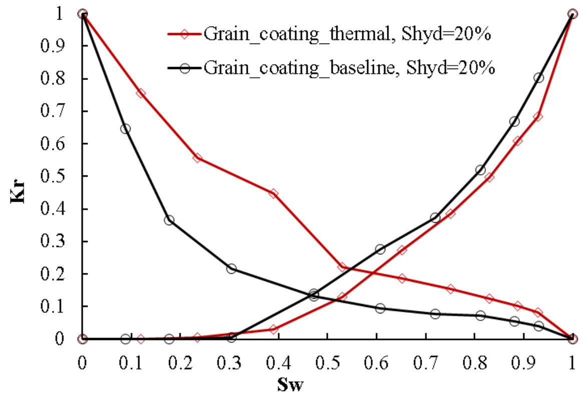

S_{hyd}=20%

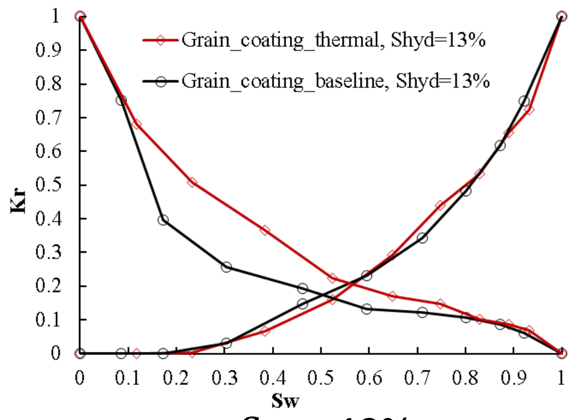

S_{hyd}=13%

K_{r} vs S_{w} comparisons

Pore-filling

Grain-coating

Conclusion

- Concluding remarks
  - Uniform dissociation in baseline model obscures the formation of hydrate-free zone, making capillarity impact and Jamin effect on fluid transport dependent solely on S_{hyd}
  - The coupling of mass and heat transfer typically results in the creation of a hydrate-free zone, causing the redistribution of fluid under capillary effects, which significantly impacts the $K_{\mathrm{r}} - S_{\mathrm{hyd}}$ relation
  - Gas is prone to occupy the hydrate-free zone under capillary force as the non-wetting phase, leading to a significant increase in $K_{\mathrm{r,g}}$ values compared to those obtained from baseline models
  - Considerable deviations can be found by comparing the $K_{\mathrm{r}} - S_{\mathrm{w}}$ relations obtained from coupled and baseline models
  - Gas bubble transport in HBS is mostly impeded by the Jamin effect, which prevents the formation of a continuous gas stream. Therefore, it is crucial to mitigate this effect during production to facilitate efficient gas extraction

References

- Methane clathrate - Wikipedia
- Ren, X., Guo, Z., Ning, F., & Ma, S. (2020). Permeability of hydrate-bearing sediments. Earth-Science Reviews, 202, 103100.
- BOSWELL, R., & SEOL, Y. (2009). Methane Hydrate, Fire in the Ice: Energy Potential and Environmental Implications. GIT laboratory journal Europe, 13(9-10), 14-15.
- Lee, J. Y., Ryu, B. J., Yun, T. S., Lee, J., & Cho, G. C. (2011). Review on the gas hydrate development and production as a new energy resource. KSCE Journal of Civil Engineering, 15, 689-696
- Malinverno, A., Kastner, M., Torres, M. E., & Wortmann, U. G. (2008). Gas hydrate occurrence from pore water chlorinity and downhole logs in a transect across the northern Cascadia margin (Integrated Ocean Drilling Program Expedition 311). Journal of Geophysical Research: Solid Earth, 113(B8).
- MH21-S R&D consortium--Fundamental Technology-- (mh21japan.gr.jp)
- Jacqmin, D. (1999). Calculation of two-phase Navier–Stokes flows using phase-field modeling. Journal of computational physics, 155(1), 96-127.
- Geier, M., Fakhari, A., & Lee, T. (2015). Conservative phase-field lattice Boltzmann model for interface tracking equation. Physical Review E, 91(6), 063309.
- Verdier, W., Kestener, P., & Cartalade, A. (2020). Performance portability of lattice Boltzmann methods for two-phase flows with phase change. Computer Methods in Applied Mechanics and Engineering, 370, 113266.
- Allen, S. M., & Cahn, J. W. (1979). A microscopic theory for antiphase boundary motion and its application to antiphase domain coarsening. Acta metallurgica, 27(6), 1085-1095.
- Aursjø, O., Løvoll, G., Knudsen, H. A., Flekkøy, E. G., & Måløy, K. J. (2011). A direct comparison between a slow pore scale drainage experiment and a 2D lattice Boltzmann simulation. Transport in porous media, 86, 125-134.

References

- Karani, H., & Huber, C. (2015). Lattice Boltzmann formulation for conjugate heat transfer in heterogeneous media. Physical Review E, 91(2), 023304.
- Dai, S., Kim, J., Xu, Y., Waite, W. F., Jang, J., Yoneda, J., Collett, T. S., & Kumar, P. (2019). Permeability anisotropy and relative permeability in sediments from the National Gas Hydrate Program Expedition 02, offshore India. Marine and Petroleum Geology, 108, 705-713.
- Li, X., Pu, C., Chen, X., Huang, F., & Zheng, H. (2021). Study on frequency optimization and mechanism of ultrasonic waves assisting water flooding in low-permeability reservoirs. Ultrasonics Sonochemistry, 70, 105291.
- Moridis, G. J. (2012). TOUGH+ HYDRATE v1. 2 User's manual: A code for the simulation of system behavior in hydrate-bearing geologic media.
- Kang, Q., Lichtner, P. C., & Zhang, D. (2006). Lattice Boltzmann pore-scale model for multicomponent reactive transport in porous media. Journal of Geophysical Research: Solid Earth, 111(B5).